Electronic Supplementary Material (ESI) for Journal of Materials Chemistry C.

Supporting Information

Proton-conductive materials formed by coumarin photocrosslinked ionic liquid crystal dendrimers

Alberto Concellón,[a] Ting Liang,[b] Albertus P. H. J. Schenning,[b,c] José Luis Serrano,[d] Pilar Romero,[,a] and Mercedes Marcos,*[,a]*

[a] Instituto de Ciencia de Materiales de Aragón, Departamento de Química Orgánica, Universidad de Zaragoza-CSIC, 50009, Zaragoza, Spain.

[b] Department of Functional Organic Materials and Devices, Chemical Engineering and Chemistry, Eindhoven University of Technology, De Rondom 70, 5612 AP, Eindhoven, The Netherlands

[c] Institute for Complex Molecular Systems (ICMS), Eindhoven University of Technology, P. O. Box 513, 5600 MB, Eindhoven, The Netherlands.

[d] Instituto de Nanociencia de Aragón, Departamento de Química Orgánica, Universidad de Zaragoza, 50009, Zaragoza, Spain.

Table of Contents

1. **Materials and methods** S3

2. **Experimental Procedures**

2.1. Synthesis of the coumarin functional units S5

2.2. Synthesis of the bifunctional dendron Ac-ChCou S6

2.3. Synthesis of the ionic hybrid dendrimers S8

3. **Supplementary Material**

3.1. FTIR and NMR characterization S11

3.2. POM textures S13

3.3 Nyquist plots S13

3.4. Optical and fluorescent properties S14

1. MATERIALS AND METHODS

Poly(amidoamine) dendrimers (PAMAM) were purchased from Dendritech, Inc. Cholesteryl hemisuccinate and the rest of reagents were purchased from Sigma-Aldrich and used as received without further purification. Anhydrous THF and DCM were purchased from Scharlab and dried using a solvent purification system. Benzyl 2,2'-bis(hydroxymethyl)propanoate was prepared following a previously reported procedure.[1] The chemical structures of all the compunds were confirmed FTIR spectroscopy, one dimensional ^{1}H and ^{13}C NMR spectroscopy and two dimensional ^{1}H-^{1}H COSY, ^{1}H-^{13}C HSQC and ^{1}H-^{13}C HMBC experiments, MALDI-TOF mass spectroscopy and elemental analysis.

FTIR spectra were obtained on a Bruker Vertex 70 FT-IR spectrophotometer using KBr pellets. Solution NMR experiments were carried out on Bruker Avance spectrometers operating at 400 MHz for ^{1}H and 100 MHz for ^{13}C, using standard pulse sequences. Chemical shifts are given in ppm relative to TMS and this was used as internal reference. Elemental analysis was performed using a Perkin-Elmer 2400 microanalyzer. MALDI-TOF MS was performed on an Autoflex mass spectrometer (Bruker Daltonics) using dithranol as matrix.

Solid-state NMR experiments were performed in a Bruker Avance III WB400 spectrometer using a double resonance (^{1}H-X) probe with a rotor of 4 mm or 2.5 mm diameter, and the spinning frequency was set to 12 kHz or 20 kHz, respectively. For the former, the ^{1}H and ^{13}C π/2 pulse length were 3 and 4.3 μs, respectively, the CP contact time was 3 ms and the recycle delay was 7 s. For the latter, the ^{1}H and ^{13}C pulse length were 8 and 5.7 μs, respectively, the CP contact time was 1.5 ms and the recycle delay was 5 s. The pulse sequence employed consisted of ramped cross-polarization with spinal-64 decoupling. Data were acquired at 298 K and chemical shifts are referenced to TMS using adamantane (^{13}C: $\delta = 29.45$ ppm) as secondary standard.

Mesogenic behavior was investigated by polarized-light optical microscopy (POM) using an Olympus BH-2 polarizing microscope fitted with a Linkam THMS600 hot stage.

Thermogravimetric analysis (TGA) was performed using a Q5000IR from TA instruments at heating rate of 10 ^{o}C min^{-1} under a nitrogen atmosphere. Thermal transitions were determined by differential scanning calorimetry (DSC) using a DSC Q2000 from TA instruments with powdered samples (2−5 mg) sealed in aluminum pans. Glass transition temperatures (T_g) were determined at the half height of the baseline jump, and first order transition temperatures were read at the maximum of the corresponding peak.

---

[1] H. Ihre, A. Hult, J. M. J. Fréchet and I. Gitsov, *Macromolecules* **1998,** 31, 4061-4068

X-ray diffraction (XRD) was performed with a Ganesha lab instrument equipped with a GeniX-Cu ultralow divergence source producing X-ray photons with a wavelength of 1.54 Å and a flux of $1 \cdot 10^{8}$ ph·s^{-1}. Scattering patterns were collected using a Pilatus 300 K silicon pixel detector. The beam center and the q range were calibrated using the diffraction peaks of silver behenate. Powdered samples were placed in Lindemann glass capillaries (1 mm diameter).

UV-Vis absorption spectra were recorded on an ATI-Unicam UV4-200 spectrophotometer. Fluorescence measurements were performed using a Perkin-Elmer LS 50B fluorescence spectrophotometer.

Electrochemical impedance spectroscopy was recorded on an Autolab potentiostat equipped with a temperature controller in the frequency range from 1 Hz to 1 MHz (applied voltage: 10 mV). The conductivities were studied as a function of temperature between 30 ºC and 150 ºC with 5 ºC intervals. For the preparation of the cells for ionic conductivities, the appropriate amount of the ionic dendrimer was placed on an ITO electrode that was sandwiched with another ITO electrode controlling the thickness by using glass spacers (20μm). The cell was heated up to a few degrees above the melting point of the liquid crystal and the cell was pressed to obtain the thin film.

After the preparation of the cell, a random orientation of the layers (SmA) or columns (Col$_h$) was observed between electrodes. Smectic samples were mechanically sheared within the cell in order to obtain a planar alignment of the layers (smectic layers aligned perpendicular to the electrodes). On the other hand, homeotropic alignment of the columnar mesophase was attainable after slow cooling down to room temperature (0.05 ºC·min^{-1}) from the isotropic liquid.

The impedance spectrum can be modeled as an equivalent circuit and divided into imaginary (Z'') and real (Z') components. The resistance (R_b) was estimated from the intersection of the real axis (Z') and the semicircle of the impedance spectrum. The proton conductivities σ (S·cm^{-1}) were calculated with the formula:

$$\sigma = {}^{d}\!/(R_b \cdot A)$$

where d (cm) is the thickness of the film, A (cm^2) is the area of the film and R_b (Ω) is the resistance of the sample.

Photocrosslinking of coumarin units (photodimerization) was carried out by exposing the aligned LC system to 365 nm LED light (ThorsLab) for 30 min.

2. EXPERIMENTAL PROCEDURES

2.1. Synthesis of the coumarin functional unit

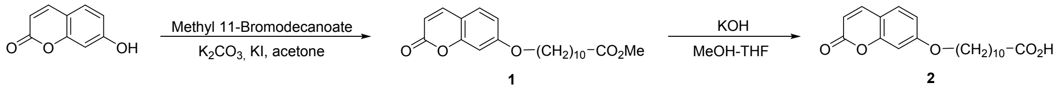

Methyl 11-[(2-oxo-2H-chromen-7-yl)oxy] undecanoate (1). A mixture of 7-hydroxy-2H-chromen-2-one (3 g, 18.5 mmol), methyl 11-bromoundecanoate (5.68 g, 20.35 mmol), anhydrous potassium carbonate (5.11 g, 37.00 mmol) and a teaspoon of KI in acetone (175 mL) was stirred and heated to reflux for 12 h. The reaction was allowed to cool down to room temperature and the solvent was evaporated under reduced pressure. The residue was dissolved in dichloromethane and washed with water and brine. The organic layer was dried over anhydrous magnesium sulfate and the solvent was evaporated. The crude product was recrystallized with ethanol. Yield: 93%. IR (KBr, ν, cm^{-1}): 2923 (C-H), 1744 (C=O), 1612, 1463 (Ar), 1232, 1126 (C-O). ^{1}H NMR ($CDCl_3$, 400 MHz, δ, ppm): 7.63 (d, *J*= 9.4 Hz, 1H), 7.6 (d, *J*= 8.5 Hz, 1H), 6.88-6.76 (m, 2H), 6.24 (d, *J*= 9.5 Hz, 1H), 4.00 (t, *J*= 6.5 Hz, 2H), 3.66 (s, 3H), 2.30 (t, *J*= 7.5 Hz, 2H), 1.85-1.74 (m, 2H), 1.67-1.55 (m, 2H), 1.51-1.21 (m, 12H). ^{13}C NMR ($CDCl_3$, 100 MHz, δ, ppm): 176.53, 162.58, 161.47, 156.07, 143.61, 128.83, 113.16, 113.05, 112.50, 101.46, 68.79, 51.60, 34.24, 29.58, 29.47, 29.43, 29.35, 29.26, 29.10, 26.07, 25.07.

11-[(2-Oxo-2H-chromen-7-yl)oxy] undecanoic acid (2). An aqueous solution of potassium hydroxide (5.45 g, 10 mL) was added to a solution of methyl 11-[(2-oxo-2H-chromen-7-yl)oxy] undecanoate (**1**) (4.5 g, 12.48 mmol) in methanol and tetrahydrofuran (50 mL and 5 mL, respectively). The mixture was stirred and heated under reflux for 2 h. Then the crude product was precipitated by addition of concentrated hydrochloric acid until pH 2 and it was filtered. The product was recrystallized in ethanol. Yield: 91%. IR (KBr, ν, cm^{-1}): 3133 (O-H), 1719, 1699 (C=O), 1619 1508, 1466 (Ar), 1205, 1139 (C-O). ^{1}H NMR ($CDCl_3$, 400 MHz, δ, ppm): 7.63 (d, *J*= 9.5 Hz, 1H), 7.35 (d, *J*= 8.4 Hz, 1H), 6.87-6.77 (m, 2H), 6.24 (d, *J*= 9.4 Hz, 1H), 4.00 (t, *J*= 7.0 Hz, 2H), 2.34 (t, *J*= 7.5 Hz, 2H), 1.87-1.75 (m, 2H), 1.68-1.58 (m, 2H), 1.51-1.22 (m, 12H). ^{13}C NMR ($CDCl_3$, 100 MHz, δ, ppm): 179.23, 162.59, 161.55, 156.06, 143.65, 128.83, 113.19, 113.03, 112.51, 101.47, 68.80, 34.05, 29.55, 29.43, 29.39, 29.32, 29.16, 29.08, 26.05, 24.81.

2.2. Synthesis of the bifunctional dendron Ac-ChCou

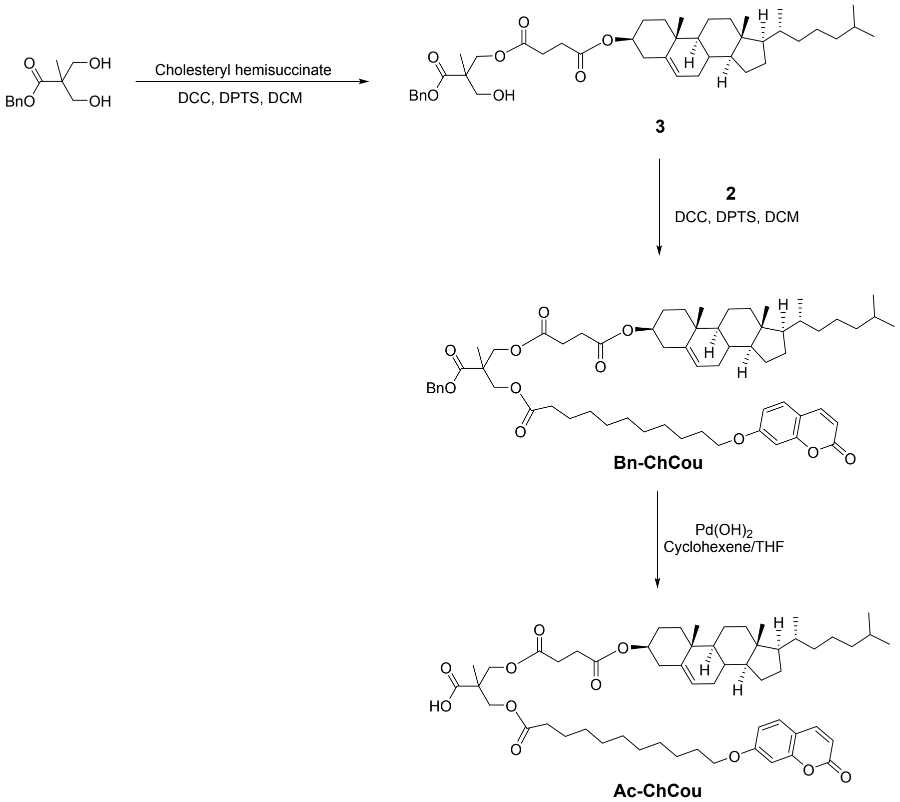

Monofunctionalized dendron (3). Benzyl 2,2'-bis(hydroxymethyl)propanoate (1.00 g, 4.46 mmol), cholesteryl hemisuccinate (2.17 g, 4.46 mmol) and (N,N'-dimethylamino)pyridinium *p*-toluenesulfonate (0.70 g, 2.23 mmol) were dissolved in dry dichloromethane (100 mL). The reaction flask was cooled in an ice bath and flushed with argon, then *N,N'*-dicyclohexylcarbodiimide (1.01 g, 4.91 mmol) was added dropwise. The mixture was stirred at RT for 24 h under argon atmosphere. The white precipitate was filtered off and washed with dichloromethane. The solvent was evaporated and the crude product was purified by flash column chromatography on silica gel using dichloromethane as eluent and gradually changing the composition of the eluent to dichloromethane/ethyl acetate (19:1). Yield: 66%. IR (KBr, v, cm^{-1}): 3516 (OH), 2954 (C-H), 1722 (C=O), 1254, 1055 (C-O).^{1}H NMR (CDCl$_3$, 400 MHz, δ, ppm): 7.41-7.28 (m, 5H), 5.36 (d, *J*= 3.6 Hz, 1H), 5.20 (d, *J*= 12.4 Hz, 1H), 5.16 (d, *J*= 12.4 Hz, 1H), 4.68-4.54 (m, 1H), 4.39 (d, *J*= 11.2 Hz, 1H), 4.25 (d, *J*= 11.2 Hz, 1H), 3.77-3.65 (m, 2H), 2.60-2.51 (m, 4H), 2.31 (d, *J*= 7.7 Hz, 2H), 2.06-0.81 (m, 41H), 0.68 (s, 3H). ^{13}C NMR (CDCl$_3$, 100 MHz, δ, ppm): 174.31, 172.63, 171.72, 139.64, 135.78, 128.75, 128.47, 128.15, 122.91, 74.64, 66.83, 66.05, 65.00, 56.82, 56.26, 50.14, 48.43, 42.44, 39.86, 39.65, 38.18, 37.08, 36.71, 36.32, 35.93, 32.03, 31.98, 29.49, 29.18, 28.37, 28.15, 27.85, 24.42, 23.96, 22.96, 22.71, 21.16, 19.44, 18.85, 17.71, 11.99.

Bifunctionalized dendron Bn-ChCou. 11-[(2-Oxo-2H-chromen-7-yl)oxy] undecanoic acid (**2**) (0.96 g, 2.77 mmol), the monofunctional dendron (**3**) (1.75 g, 2.53 mmol) and (N,N'-dimethylamino)pyridinium *p*-toluenesulfonate (0.39 g, 1.26 mmol) were dissolved in dry dichloromethane (75 mL). The reaction flask was cooled in an ice bath and flushed with argon, then *N,N'*-dicyclohexylcarbodiimide (0.63 g, 3.03 mmol) was added dropwise. The mixture was stirred at RT for 24 h under argon atmosphere. The white precipitate was filtered off and washed with dichloromethane. The solvent was evaporated and the crude product was purified by flash column chromatography on silica gel using dichloromethane as eluent and gradually changing the composition of the eluent to dichloromethane/ethyl acetate (19:1). Yield: 90%. IR (KBr, ν, cm^{-1}): 2934 (C-H), 1741 (C=O), 1613, 1467 (Ar), 1231, 1156 (C-O). ^1H NMR ($CDCl_3$, 400 MHz, δ, ppm): 7.63 (d, *J*= 9.4 Hz, 1H), 7.40-7.27 (m, 6H), 6.86-6.77 (m, 2H), 6.24 (d, *J*= 9.5 Hz, 1H), 5.40-5.30 (m, 1H), 5.16 (s, 2H), 4.66-4.54 (m, 1H), 4.31-4.16 (m, 4H), 4.00 (t, *J*= 6.5 Hz, 2H), 2.60-2.48 (m, 4H), 2.30 (d, *J*= 7.7 Hz, 2H), 2.22 (t, *J*= 7.6 Hz, 2H), 2.04-0.80 (m, 54H), 0.67 (s, 3H). ^{13}C NMR ($CDCl_3$, 100 MHz, δ, ppm): 173.35, 172.69, 171.94, 171.56, 162.59, 161.41, 156.10, 143.57, 139.71, 135.76, 128.82, 128.72, 128.47, 128.27, 122.86, 113.15, 113.08, 112.51, 101.49, 74.55, 68.81, 66.94, 65.77, 65.43, 56.84, 56.29, 50.17, 46.55, 42.46, 39.88, 39.66, 38.20, 37.10, 36.72, 36.33, 35.93, 34.18, 32.04, 32.00, 29.62, 29.51, 29.46, 29.36, 29.24, 29.13, 28.37, 28.16, 27.88, 26.10, 24.94, 24.42, 23.98, 22.96, 22.70, 21.17, 19.45, 18.86, 17.91, 12.00.

Bifunctionalized dendron Ac-ChCou. The dendron with benzyl ester group (**Bn-ChCou**) and $Pd(OH)_2/C$ (20% wt.) were dissolved in a mixture of THF-cyclohexene (1:3) under reflux. After 12 h, the catalyst was filtered off using Celite® and carefully washed with dichloromethane. The solvent was evaporated and the crude product was purified by flash column chromatography on silica gel using dichloromethane as eluent and gradually changing the composition of the eluent to ethyl acetate. Yield: quantitative. IR (KBr, ν, cm^{-1}): 3228 (OH), 3044 (=C-H), 2932 (C-H), 1741, 1730, 1683 (C=O), 1604, 1507, 1466 (Ar), 1252, 1165 (C-O). ^1H NMR ($CDCl_3$, 400 MHz, δ, ppm): 7.63 (d, *J*= 9.5 Hz, 1H), 7.36 (d, *J*= 8.5 Hz, 1H), 6.89-6.75 (m, 2H), 6.24 (d, *J*= 9.5 Hz, 1H), 5.40-5.30 (m, 1H), 4.68-4.54 (m, 1H), 4.32-4.18 (m, 4H), 4.01 (t, *J*= 6.5 Hz, 2H), 2.69-2.54 (m, 4H), 2.36-2.25 (m, 4H), 2.04-0.80 (m, 54H), 0.67 (s, 3H). ^{13}C NMR ($CDCl_3$, 100 MHz, δ, ppm): 176.98, 173.40, 171.97, 171.65, 162.61, 161.57, 156.07, 143.65, 139.70, 128.84, 122.87, 113.20, 113.05, 112.53, 101.50, 74.62, 68.82, 65.50, 65.12, 56.83, 56.30, 50.16, 46.21, 42.46, 39.87, 39.66, 38.19, 37.10, 36.72, 36.33, 35.94, 34.22, 32.04, 32.00, 29.58, 29.48, 29.40, 29.33, 29.23, 29.19, 29.09, 28.37, 28.16, 27.87, 26.07, 24.96, 24.43, 23.99, 22.96, 22.70, 21.17, 19.45, 18.86, 17.89, 12.00. MS ($MALDI^+$, dithranol, m/z): calcd. for $C_{56}H_{82}O_{11}$, 930.6; found, 953.6 $[M+Na]^+$, 975.6 $[M-H+2Na]^+$. Anal. calcd. for $C_{56}H_{82}O_{11}$: C, 72.23%; H, 8.88%. Found: C, 72.00%; H, 8.94%.

2.3. Synthesis of the ionic hybrid dendrimers

Ionic dendrimers were prepared following the previously described methodology.[2,3] A solution of **Ac-ChCou** in dry tetrahydrofuran was added to a solution of the corresponding generation of PAMAM dendrimer, in approximately 1:1 (primary amine groups:carboxylic acid groups) stoichiometry. The mixture was ultrasonicated for 5 min, and then it was slowly evaporated at room temperature and dried in vacuum at 40^{o}C until the weight remained constant.

PAMAM4-ChCou. IR (KBr, ν, cm^{-1}): 3258 (N-H), 3069 (=C-H), 2930 (C-H), 1729, 1645 (C=O), 1611 (Ar), 1555 (COO$^{-}_{asym}$), 1406 (COO$^{-}_{sym}$), 1158 (C-O). ^{1}H NMR (CDCl3, 400 MHz, δ, ppm): 8.71-8.50 (m, 4H), 7.63 (d, *J*= 9.5 Hz, 4H), 7.35 (d, *J*= 8.6 Hz, 4H), 6.85-6.76 (m, 8H), 6.23 (d, *J*= 9.5 Hz, 4H), 5.39-5.29 (m, 4H), 4.68-4.47 (m, 4H), 4.36-4.08 (m, 16H), 4.00 (t, *J*= 6.5 Hz, 8H), 3.65-3.43 (m, 4H), 3.22-3.02 (m, 4H), 3.00-2.23 (m, 52H), 2.05-0.74 (m, 216H), 0.66 (s, 12H). ^{13}C NMR (CDCl3, 100 MHz, δ, ppm): 178.40, 173.80, 172.31, 172.02, 162.60, 161.49, 156.08, 143.65, 139.71, 128.86, 122.87, 113.16, 113.04, 112.52, 101.49, 74.62, 68.81, 68.12, 66.80, 66.15, 56.83, 56.32, 50.58 (detected by ^{1}H-^{13}C HSQC, H$_{\zeta}$-C$_{\zeta}$), 50.15, 49.98 (detected by ^{1}H-^{13}C HSQC, H$_{\varepsilon}$-C$_{\varepsilon}$), 46.59, 42.46, 39.87, 39.66, 39.28 (detected by ^{1}H-^{13}C HSQC, H$_{\eta}$-C$_{\eta}$), 39.10 (detected by ^{1}H-^{13}C HSQC, H$_{\alpha}$-C$_{\alpha}$), 38.20, 37.40 (detected by ^{1}H-^{13}C HSQC, H$_{\beta}$-C$_{\beta}$), 37.10, 36.73, 36.34, 35.95, 34.38, 32.85 (detected by ^{1}H-^{13}C HSQC, H$_{\delta}$-C$_{\delta}$), 32.05, 31.99, 29.65, 29.56, 29.47, 29.44, 29.34, 29.22, 29.13, 28.38, 28.16, 27.87, 26.10, 25.76, 25.06, 24.43, 24.02, 22.97, 22.71, 21.18, 19.45, 18.86, 18.64, 12.00.

PAMAM8-ChCou. IR (KBr, ν, cm^{-1}): 3260 (N-H), 3070 (=C-H), 2928 (C-H), 1728, 1644 (C=O), 1610 (Ar), 1555 (COO$^{-}_{asym}$), 1406 (COO$^{-}_{sym}$), 1158 (C-O). ^{1}H NMR (CDCl$_3$, 400 MHz, δ, ppm): 8.74-8.47 (m, 8H), 8.21- 8.06 (m, 4H), 7.63 (d, *J*= 9.5 Hz, 8H), 7.36 (d, *J*= 8.6 Hz, 8H), 6.89-6.74 (m, 16H), 6.24 (d, *J*= 9.5 Hz, 8H), 5.43-5.27 (m, 8H), 4.69-4.49 (m, 8H), 4.39-4.09 (m, 32H), 4.00 (t, *J*= 6.5 Hz, 16H), 3.62-3.45 (m, 16H), 3.37-3.04 (m, 24H), 2.90-2.19 (m, 120H), 2.07-0.76 (m, 432H), 0.66 (s, 24H). ^{13}C NMR (CDCl$_3$, 100 MHz, δ, ppm):178.02, 173.74, 172.25, 171.90, 162.59, 161.51, 156.06, 143.66, 139.70, 128.85, 122.86, 113.16, 113.03, 112.51, 101.48, 74.59, 68.80, 56.82, 56.30, 52.28 (detected by ^{1}H-^{13}C HSQC, H$_{\zeta}$-C$_{\zeta}$), 50.18 (detected by ^{1}H-^{13}C HSQC, H$_{\varepsilon}$-C$_{\varepsilon}$), 50.14, 42.45, 39.86, 39.65, 39.34 (detected by ^{1}H-^{13}C HSQC, H$_{\alpha}$-C$_{\alpha}$), 38.18, 37.75 (detected by ^{1}H-^{13}C HSQC, H$_{\eta}$-C$_{\eta}$), 37.40 (detected by ^{1}H-^{13}C HSQC, H$_{\beta}$-C$_{\beta}$), 37.09, 36.72, 36.33, 35.94, 34.35, 34.10 (detected by ^{1}H-^{13}C HSQC, H$_{\delta}$-C$_{\delta}$), 32.04, 31.98, 29.63, 29.55, 29.51, 29.45, 29.42, 29.32, 29.11, 28.37, 28.15,

---

[2] V. Chechik, M. Zhao, R. M. Crooks,. *J. Am. Chem. Soc.* **1999**, *121*, 4910.

[3] R. Martín-Rapún, M. Marcos, A. Omenat, J. Barberá, P. Romero, J. L. Serrano, *J. Am. Chem. Soc.* **2005,** *127*, 7397.

27.86, 26.09, 25.03, 24.42, 24.01, 22.96, 22.71, 21.17, 19.45, 18.86, 18.54, 11.99.

PAMAM16-ChCou. IR (KBr, ν, cm^{-1}): 3261 (N-H), 3069 (=C-H), 2929 (C-H), 1729, 1645 (C=O), 1610 (Ar), 1555 (COO$^{-}_{asym}$), 1406 (COO$^{-}_{sym}$), 1158 (C-O). ^{1}H NMR (CDCl$_3$, 400 MHz, δ, ppm): 8.82-8.45 (m, 16H), 8.27-7.96 (m, 12H), 7.63 (d, *J*= 9.5 Hz, 17H), 7.35 (d, *J*= 8.6 Hz, 16H), 6.87-6.74 (m, 32H), 6.23 (d, *J*= 9.5 Hz, 16H), 5.40-5.28 (m, 16H), 4.70-4.46 (m, 16H), 4.38-4.08 (m, 64H), 3.99 (t, *J*= 6.5 Hz, 32H), 3.65-3.41 (m, 32H), 3.37-3.03 (m, 56H), 2.88-2.16 (m, 264H), 2.08-0.75 (m, 864H), 0.66 (s, 48H). ^{13}C NMR (CDCl$_3$, 100 MHz, δ, ppm): 173.73, 172.26, 171.86, 162.59, 161.48, 156.05, 143.66, 139.70, 128.86, 122.84, 113.14, 113.02, 112.51, 101.48, 74.55, 68.80, 68.10, 66.64, 66.05, 56.82, 56.31, 52.30 (detected by ^{1}H-^{13}C HSQC, H$_{\zeta}$-C$_{\zeta}$), 50.36 (detected by ^{1}H-^{13}C HSQC, H$_{\varepsilon}$-C$_{\varepsilon}$), 50.14, 46.51, 42.44, 39.86, 39.64, 39.56 (detected by ^{1}H-^{13}C HSQC, H$_{\alpha}$-C$_{\alpha}$), 38.19, 37.78 (detected by ^{1}H-^{13}C HSQC, H$_{\eta}$-C$_{\eta}$), 37.52 (detected by ^{1}H-^{13}C HSQC, H$_{\beta}$-C$_{\beta}$), 37.09, 36.71, 36.33, 35.93, 34.35, 34.17 (detected by ^{1}H-^{13}C HSQC, H$_{\delta}$-C$_{\delta}$), 31.98, 29.65, 29.56, 29.47, 29.33, 29.12, 28.36, 28.15, 27.86, 26.10, 25.74, 25.04, 24.42, 24.01, 22.96, 22.70, 21.16, 19.45, 18.86, 18.65, 11.99.

PAMAM32-ChCou. IR (KBr, ν, cm^{-1}): 3260 (N-H), 3069 (=C-H), 2929 (C-H), 1729, 1645 (C=O), 1610 (Ar), 1554 (COO$^{-}_{asym}$), 1405 (COO$^{-}_{sym}$), 1160 (C-O). ^{1}H NMR (CDCl$_3$, 400 MHz, δ, ppm): 8.72-8.38 (m, 32H), 8.29-7.96 (m, 28H), 7.63 (d, *J*= 9.5 Hz, 32H), 7.35 (d, *J*= 8.6 Hz, 32H), 6.85-6.74 (m, 64H), 6.22 (d, *J*= 9.5, 32H), 5.39-5.28 (m, 32H), 4.64-4.50 (m, 32H), 4.36-4.05 (m, 128H), 3.99 (t, *J*= 6.5 Hz, 64H), 3.65-3.37 (m, 64H), 3.37-3.00 (m, 120H), 2.93-2.19 (m, 552H), 2.09-0.75 (m, 1728H), 0.66 (s, 96H). ^{13}C NMR (CDCl$_3$, 100 MHz, δ, ppm): 178.59, 173.82, 172.35, 171.93, 162.61, 161.48, 156.08, 143.66, 139.73, 128.88, 122.85, 113.15, 113.04, 112.54, 101.52, 74.58, 68.82, 66.49, 66.26, 56.85, 56.37, 52.58 (detected by ^{1}H-^{13}C HSQC, H$_{\zeta}$-C$_{\zeta}$), 50.33 (detected by ^{1}H-^{13}C HSQC, H$_{\varepsilon}$-C$_{\varepsilon}$), 50.18, 46.60, 42.47, 39.89, 39.69 (detected by ^{1}H-^{13}C HSQC, H$_{\alpha}$-C$_{\alpha}$), 39.67, 38.21, 37.80 (detected by ^{1}H-^{13}C HSQC, H$_{\eta}$-C$_{\eta}$), 37.75 (detected by ^{1}H-^{13}C HSQC, H$_{\beta}$-C$_{\beta}$), 37.12, 36.74, 36.36, 35.96, 34.38, 34.25 (detected by ^{1}H-^{13}C HSQC, H$_{\delta}$-C$_{\delta}$), 32.05, 29.85, 29.67, 29.59, 29.49, 29.36, 29.27, 29.15, 28.38, 28.16, 27.88, 26.12, 25.06, 24.44, 24.05, 22.96, 22.71, 21.19, 19.46, 18.88, 18.63, 12.01.

PAMAM64-ChCou. IR (KBr, ν, cm^{-1}): 3260 (N-H), 3069 (=C-H), 2929 (C-H), 1729, 1645 (C=O), 1610 (Ar), 1555 (COO$^{-}_{asym}$), 1406 (COO$^{-}_{sym}$), 1158 (C-O). ^{1}H NMR (CDCl$_3$, 400 MHz, δ, ppm): 8.84-8.48 (m, 64H), 8.23-7.94 (m, 60H), 7.63 (d, *J*= 9.5 Hz, 64H), 7.35 (d, *J*= 8.6 Hz, 64H), 6.90-6.69 (m, 128H), 6.23 (d, *J*= 9.5 Hz, 64H), 5.42-5.26 (m, 64H), 4.69-4.49 (m, 64H), 4.39-4.04 (m, 256H), 3.97 (t, *J*= 6.5 Hz, 128H), 3.67-2.99 (m, 376H), 2.96-2.13 (m, 1128H), 2.10-0.75 (m, 3456H), 0.70 (s, 192H). ^{13}C NMR (CDCl$_3$, 100 MHz, δ, ppm): 178.08, 173.70, 172.23, 171.82, 162.59, 161.49, 156.05, 143.68, 139.69, 128.87, 122.84, 113.14, 113.01, 112.51, 101.48, 74.54, 68.80, 68.10, 66.53, 56.81, 56.32, 52.14 (detected by ^{1}H-^{13}C HSQC, H_{ζ}-C_{ζ}), 50.20 (detected by ^{1}H-^{13}C HSQC, H_{ε}-C_{ε}), 50.14, 46.49, 42.44, 39.86, 39.64, 39.41 (detected by ^{1}H-^{13}C HSQC, H_{α}-C_{α}), 38.19, 37.57 (detected by ^{1}H-^{13}C HSQC, H_{η}-C_{η}), 37.52 (detected by ^{1}H-^{13}C HSQC, H_{β}-C_{β}), 37.09, 36.71, 36.33, 35.94, 34.34, 31.98, 29.65, 29.57, 29.47, 29.33, 29.13, 28.37, 28.15, 27.86, 26.10, 25.74, 25.04, 24.42, 24.02, 22.96, 22.70, 21.17, 19.45, 18.86, 18.59, 11.99.

3. SUPPLEMENTARY MATERIAL

3.1. FTIR and NMR characterization

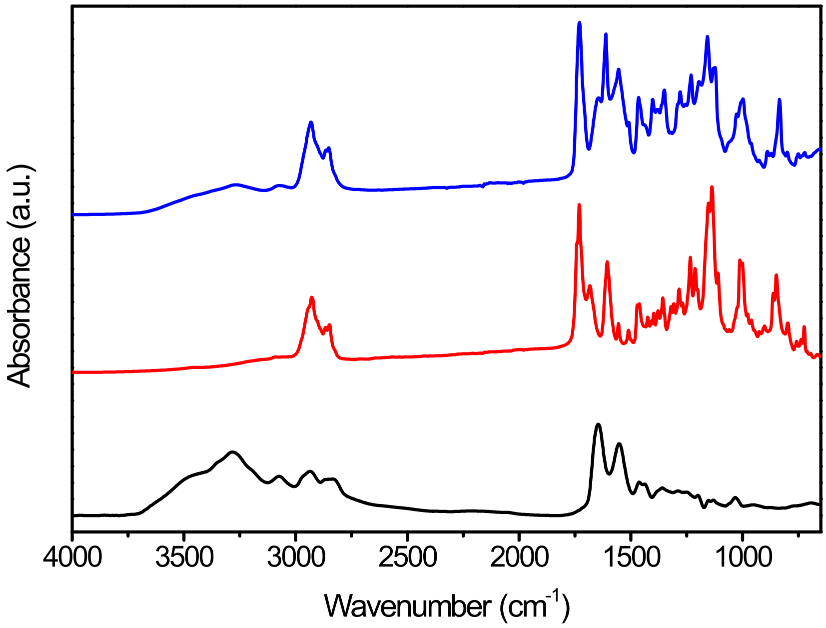

Figure S1. FTIR spectra (C=O st. region) of **PAMAM16** (black line), **Ac-ChCou** (blue line), and **PAMAM16-ChCou** (red line)

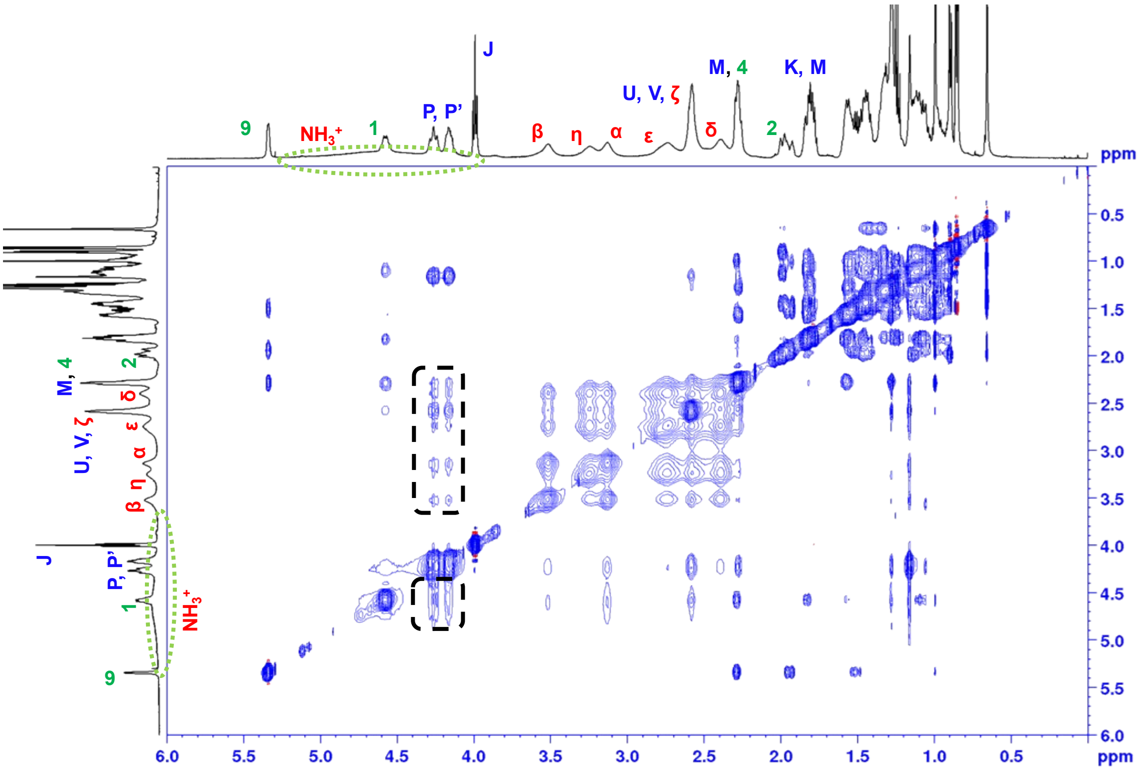

Figure S2. ^{1}H-^{1}H NOESY spectrum of **PAMAM32-ChCou** (CDCl$_3$, 298 K, t_{mix} = 200 ms).

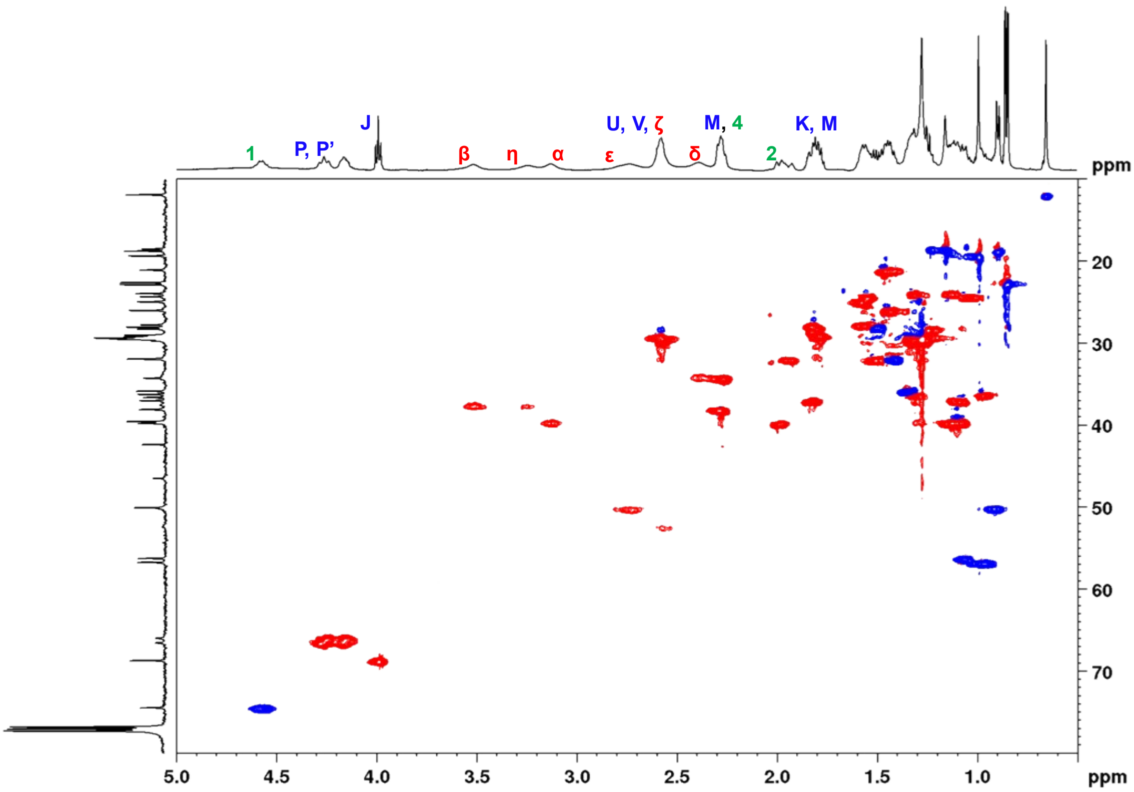

Figure S3. ^{1}H-^{13}C HSQC spectrum of **PAMAM32-ChCou** ($CDCl_3$, 298 K).

3.2. POM textures

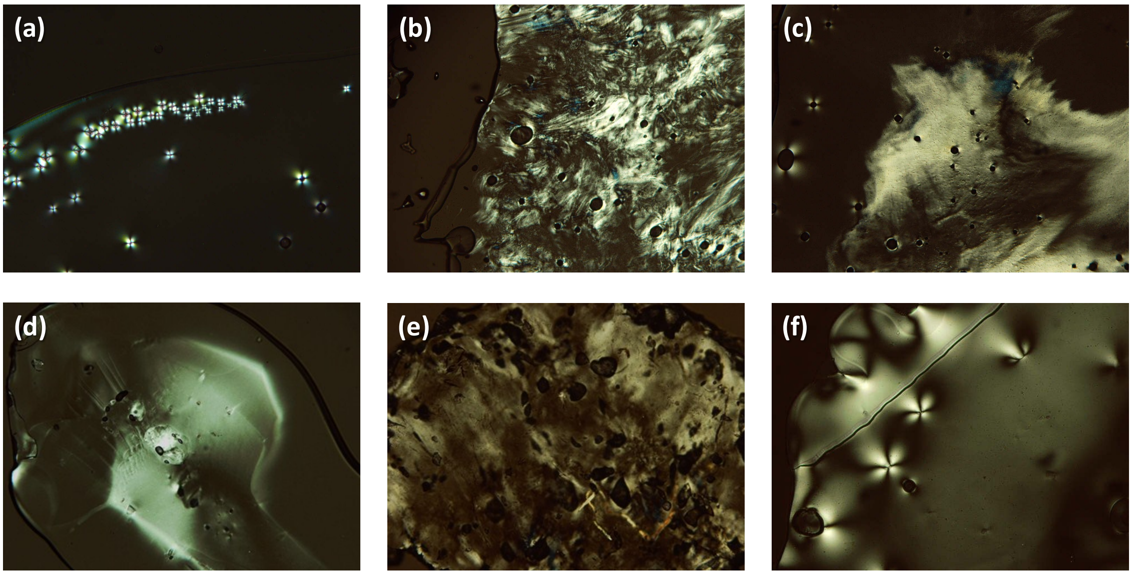

Figure S4. POM microphotographs observed in the cooling process at room temperature for: **(a) Ac-ChCou**, **(b) PAMAM4-ChCou**, **(c) PAMAM8-ChCou**, **(d) PAMAM16-ChCou**, **(e) PAMAM32-ChCou**, and **(f) PAMAM64-ChCou**.

3.3. Nyquist plots

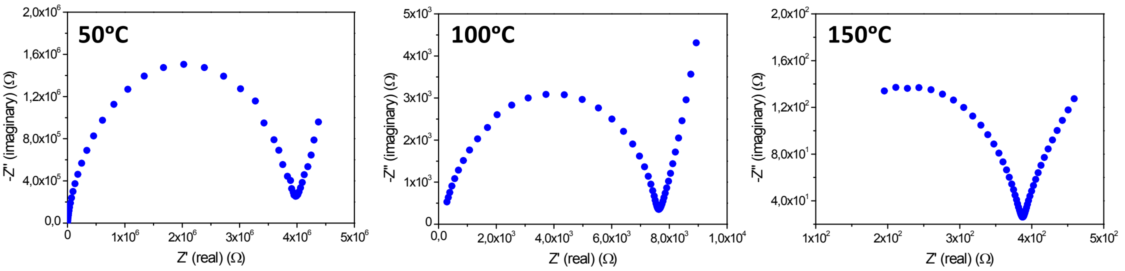

Figure S5. Nyquist plots of **PAMAM64-ChCou** at 50ºC, 100ºC and 150ºC.

3.4. Optical and fluorescent properties

The ionic dendrimers present identical absorption spectra in THF solution with a band at 323 nm related to the π–π* transition of the coumarin units. The UV-Vis absorption spectra in solid thin films showed that the absorption band was broader respect to the corresponding THF solutions, due to aggregation of the ionic dendrimers. The fluorescence emission spectra in THF solution exhibit one band at 384 nm. The fluorescence quantum yields (Φ) of the ionic dendrimers were also measured with anthracene (Φ = 0.27 in ethanol) as standard, obtaining moderate quantum yield values in the range of 0.45-0.58. In general, the quantum yields increase as the generation increases. The fluorescence emission in solid thin film was also recorded. Compared to the data from THF solutions, the emission peak appeared broader and red-shifted by ca. 50 nm.

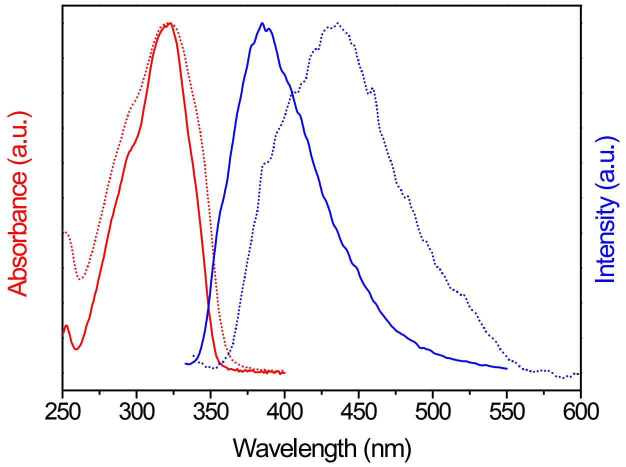

Figure S6. Absorption (red) and emission (blue) spectra of **PAMAM64-ChCou** in THF solution (solid line) and in thin film (dot line).

Table S1. Photophysical data

	λ_{abs}^{THF} (log ε)[a]	$\lambda_{abs}^{film\ a}$	$\lambda_{em}^{THF\ b}$	Φ [c]
Ac-ChCou	324 (4.13)	323	434	0.48
PAMAM4-ChCou	323 (4.72)	323	434	0.45
PAMAM8-ChCou	323 (5.03)	323	434	0.46
PAMAM16-ChCou	324 (5.32)	323	434	0.51
PAMAM32-ChCou	323 (5.61)	323	434	0.58
PAMAM64-ChCou	323 (5.94)	323	434	0.56

[a] Maximum of the absorption band in nm (ε: extinction coefficient in M^{-1} cm^{-1}). [b] Maximum of the emission band in nm. [c] Quantum yields in THF relative to anthracene (Φ=0.27 in ethanol)